Atmospheric Environment 77 (2013) 757–766

Contents lists available at SciVerse ScienceDirect

Atmospheric Environment

journal homepage: www.elsevier.com/locate/atmosenv

Variation trends and influencing factors of total gaseous mercury in the Pearl River Delta—A highly industrialised region in South China influenced by seasonal monsoons

Laiguo Chen [a,*], Ming Liu [a,b], Zhencheng Xu [a], Ruifang Fan [b], Jun Tao [a], Duohong Chen [c], Deqiang Zhang [d], Donghai Xie [e], Jiaren Sun [a]

[a] Urban Environment and Ecology Research Center, South China Institute of Environmental Sciences (SCIES), Ministry of Environmental Protection (MEP), Guangzhou 510655, China
[b] College of Life Science, South China Normal University, Guangzhou 510631, China
[c] State Environmental Protection Key Laboratory of Regional Air Quality Monitoring, Guangdong Environmental Monitoring Center, Guangzhou 510045, China
[d] South China Botanical Garden, Chinese Academy of Sciences, Guangzhou 510650, China
[e] Hainan Research Academy of Environmental Sciences, Haikou 570206, China

HIGHLIGHTS

- The TGM levels were 1–2 times greater than the regional background values.
- The monsoon winds were the dominant factor controlling TGM seasonal variability.
- The TGM diurnal patterns at two sites were opposite.
- Anthropogenic emission sources contribute significantly for the TGM levels.

ARTICLE INFO

Article history:
Received 26 February 2013
Received in revised form
10 May 2013
Accepted 21 May 2013

Keywords:
Total gaseous mercury
The Pearl River Delta
Variation trend
Influencing factors

ABSTRACT

Studies on atmospheric mercury in the Pearl River Delta (PRD) region are important because of the economic relevance of this region to China, because of its economic developmental pattern and because it is a highly industrialised area influenced by the strong seasonal monsoons. Total gaseous mercury (TGM), meteorological parameters and criteria pollutant concentrations were measured at Mt. Dinghu (DH, a regional monitoring site) and Guangzhou (GZ, an urban monitoring site) in the PRD region from October 2009 to April 2010 and from November 2010 to November 2011, respectively. The ranges of daily average TGM concentrations at the DH and GZ sites were 1.87–29.9 ng m^{-3} (5.07 ± 2.89 ng m^{-3}) and 2.66–11.1 ng m^{-3} (4.60 ± 1.36 ng m^{-3}), respectively, which were far more significant than the background values in the Northern Hemisphere (1.5–1.7 ng m^{-3}), suggesting that the atmosphere in the PRD has suffered from mercury pollution. Similar TGM seasonal distributions at the two sites were observed, with a descending order of spring, winter, autumn and summer. The different seasonal monsoons were the dominant factor controlling the seasonal variability of the TGM, with variations in the boundary layer and oxidation also possibly partially contributing. Different diurnal patterns of the TGM at two sites were observed. TGM levels during the daytime were higher than those during the nighttime and were predominantly influenced by mountain and valley winds at the DH site, whereas the opposite trend was evident at the GZ site, which was primarily influenced by the boundary-layer height and O_3 concentration. During the monitoring period, the correlations between the daily TGM levels and the SO_2 and NO_2 levels at the DH site were significant ($r = 0.36$, $p < 0.001$; $r = 0.29$, $p < 0.001$), suggesting that coal-fired emission is an important source of mercury for this regional monitoring site. At the GZ site, the correlations between the daily TGM level and the NO, NO_2, CO levels were significant ($r = 0.501$, $p < 0.001$; $r = 0.579$, $p < 0.001$; $r = 0.358$, $p < 0.001$). However, TGM was partially correlated with SO_2, suggesting that the combined vehicle emissions and coal combustion were the dominant mercury

* Corresponding author.
E-mail address: 631811743@qq.com (L. Chen).

1352-2310/$ – see front matter
http://dx.doi.org/10.1016/j.atmosenv.2013.05.053

sources for this urban monitoring site. The TGM distribution figure, which related to the wind-rose pattern and the distribution figure of emission sources, indicated significant contributions from anthropogenic emission sources.

1. Introduction

Mercury has been recognised as a global pollutant. Both human activities and natural processes emit gaseous-phase mercury into the atmosphere (Pirrone et al., 2009, 2010). The amount of mercury from anthropogenic sources, predominantly due to fossil fuel-fired power plants, is 2320 t annually (Pirrone et al., 2010). The amount of total mercury emissions from China in 2005 has been estimated to be over 800 t (Pacyna et al., 2010). In 2008, coal consumption in Guangdong province was approximately 132 million tons, which continues to increase with increasing economic development and increasing oil prices (Chen et al., 2012). In the next few decades, a significant increase in anthropogenic mercury emissions in Asia (especially in China) is likely because of rapid economic and industrial development unless drastic measures are taken (Wong et al., 2006). Numerous actions, such as the Global Mercury Assessment Report (UNEP, 2002) and European Mercury Strategy, have been taken to support the achievement of the objectives set by the United Nations Environmental Program (UNEP) Governing Council, aiming at phasing out mercury use and reducing its emissions. In China, the 12th 5-year (2011–2015) plan has listed mercury as one of the heavy metals to be addressed in the integrated pollution control programme (Zheng et al., 2011).

Elevated atmospheric mercury levels in China have attracted global attentions, and some attempts have been made to predict their spatiotemporal distribution, to report the emission inventory and to model the process of atmospheric mercury in China (Dastoor and Larocque, 2004; Seigneur et al., 2004; Streets et al., 2005). Compared to the TGM concentrations reported in China, modelling results have underestimated TGM concentrations in ambient air in China. Therefore, more scientific observation data are required to clarify the discrepancy between the modelled and observed levels (Fu et al., 2009). In China, there have been relatively few long-term observational studies of TGM. These studies simultaneously focus on the east, southwest and north of China (Feng et al., 2004; Fu et al., 2008, 2009, 2012a, 2012b; Wan et al., 2009; Ci et al., 2011). To our knowledge, only two short-term field studies of TGM in the PRD have been reported (Wang et al., 2007; Li et al., 2011).

The Pearl River Delta (PRD) region is well known to be one of the most industrialised and urbanised regions in China. In 2008, the gross domestic product (GDP) of the PRD was $434.3 billion, which represented more than 83% of the GDP of Guangdong province and approximately 10% of the GDP of China (Guangdong Statistical Yearbook, 2009). Due to rapid urbanisation and industrialisation over the past two decades, a large increase in the emission of major air pollutants has contributed to deteriorating regional air, soil and water quality. Environmental pollution has become a problem of increasing concern, and studies on heavy metal have been undertaken in this region (Shi et al., 2010; Chen et al., 2012). Mercury, however, has largely been ignored in most studies of pollutants. Thus, the extent to which the PRD is contaminated with mercury is still unknown (Li et al., 2011; Chen et al., 2013).

The PRD is located in the central southern coastal part of the Guangdong province of China. The landscape consists of a flat plain between the Nanling Mountains in the north and the South China Sea to the south, and it is surrounded by high mountains to the east, west and north. This unique geographical circumstance has had significant impacts on its regional air quality (Zhang et al., 2008a). The climate is dominated by subtropical/tropical monsoon winds and rain. In the winter, the Siberian High produces strong northeasterly winds at the boundary layer along the Pacific Rim. However, in the summer, the Pacific High builds up and produces strong warm tropical air from the South Sea (Wang et al., 2003). A reasonably prevailing southerly wind and northerly winds during the summer and winter, respectively, due to monsoons in the PRD are present. It has been reported that the levels of atmospheric total gaseous mercury (TGM) in the South China Sea are tightly related to the long-range transport of air masses (Fu et al., 2010).

Given the developed economy, enormous energy demand and strong seasonal monsoons in southern China, the need for long-term TGM measurements in this region is apparent. Based on the specific physical and chemical characteristics of the mercury and the unique subtropical monsoon climatic conditions in the PRD region, significant efforts should be made to control mercury pollution in this region. This investigation aims (1) to conduct one year observations of TGM at different types of monitoring sites in the PRD and to determine the TGM variation characteristics; (2) to study the relationships between TGM, meteorological parameters and criteria air pollutants and to ascertain the factors that influence and control the variation of TGM; (3) to confirm the degree of influence of emission sources on the variation of TGM in this region.

2. Experimental methods

2.1. Sampling site

Mt. Dinghu is located in the northwest of the PRD and is a national nature reserve. The Dinghu site (DH) (E 112°32′57″, N 23°9′51″) is located at a small peak in the Dinghushan (Mt. Dinghu) Forest Ecosystem Research Station of the Chinese Academy of Sciences (CAS) (Fig. 1) without distinctly industrial emission sources within a range of 10 km. Because atmospheric pollutants in the Dinghu region predominantly come from regional atmospheric transport, some studies have regarded it as a regional atmospheric monitoring area that represents the pollution level of the entire PRD region (Yang et al., 2009; Yu et al., 2011).

Guangzhou, a typical city, is located in the centre of the rich PRD and is the provincial capital of Guangdong province. It is the central city and the third largest city in China with a population of 10 million and an urban area of 1443 km^2. The GDP of Guangzhou was $165 billion in 2010 and has continuously grown at 10%. The Guangzhou observation site (GZ) (E 113°21′17.4″, N 23°07′26.8″) was located at the Super Atmospheric Observation Station (SAOS) of the South China Institute of Environmental Sciences (SCIES) (Fig. 1), which was elevated 40 m above the ground and did not have distinctly industrial emission sources within a range of 8 km, with three main roads north, east and south of the monitoring site.

2.2. Measurements of atmospheric TGM

The campaign was performed from October 2009 to April 2010 at the DH site and from November 2010 to October 2011 at the GZ site. The TGM monitoring was performed *in situ* using an automatic mercury vapour analyser (model 2537B, Tekran, Toronto, Canada).

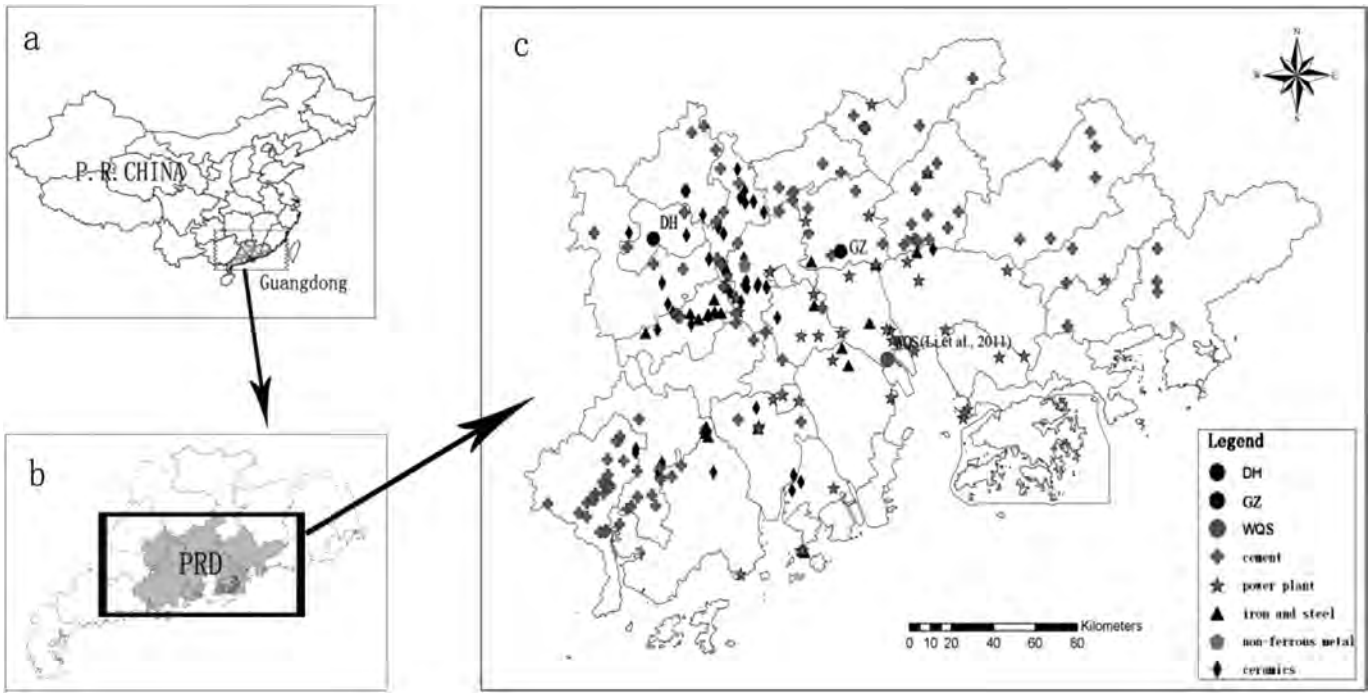

Fig. 1. Schematic showing the geographical locality of (a) the Guangdong Province in China; (b) the Pearl River Delta (PRD) region in the Guangdong Province; and (c) the sampling sites and potential source regions of atmospheric mercury.

The analyser was programmed to measure atmospheric TGM at a time resolution of 5 min and at a sampling flow rate of 1.0 L min^{-1} at Guangzhou and 1.5 L min^{-1} at Mt. Dinghu. The Tekran 2537B analyser was calibrated automatically every 25 h using the instrument's internal mercury permeation source. Manual injections were used to evaluate these automated calibrations using a saturated mercury vapour standard from an external mercury vapour source (Tekran 2505) before and after the campaign. The relative percent difference between the manual injections and the automated calibrations was less than 5%. The TGM detection limit in this operation mode is less than 0.1 ng m^{-3}.

The entire sampling period was divided into 4 seasons based on conventional meteorological classifications. The months of spring, summer, autumn and winter in the PRD are March–May, June–September, October–November and December–February, respectively.

2.3. Meteorological parameters and criteria pollutant data

Conventional meteorological data (i.e., wind speed, wind direction, temperature, relative humidity and pressure) were collected at the DH and GZ monitoring sites using a meteorological instrument (model 310, Vaisala, Finland). In addition, the ground surface temperature was also measured at the DH site. Monitoring the data for the criteria pollutants (i.e., SO_2 and NO_2) at the DH sampling site was accomplished at an atmospheric monitoring station supervised by a local environmental monitoring centre, which was approximately 1 km from our monitoring site. Criteria pollutants (i.e., SO_2, NO_2, NO, CO and O_3) at the GZ monitoring site were measured from our SAOS.

2.4. Statistical analysis

Because of the normal distribution of the data (Kolmogorov–Smirnov test, $p > 0.05$), all data were statistically processed using the independent-samples *t* test. Statistical analyses for all the data were performed using SPSS v 13.0 for Windows (SPSS, Chicago, USA). The results of the statistical tests were considered statistically significant when $p < 0.05$.

3. Results and discussion

3.1. The temporal and spatial levels of TGM in the PRD

During the monitoring period, the daily average TGM concentration ranged from 1.87 to 29.9 ng m^{-3} and from 2.66 to 11.1 ng m^{-3} at the DH and GZ sampling sites, respectively, with average values of 5.07 ± 2.89 ng m^{-3} and 4.60 ± 1.36 ng m^{-3}, respectively. Compared with other studies in China and background levels, the TGM concentrations in the PRD were obviously higher than global background levels (1.5–1.7 ng m^{-3}, Lindberg et al., 2007; Valente et al., 2007), the domestic remote sites, such as Mt. Gongga (3.98 ng m^{-3}, Fu et al., 2008), Mt. Waliguan (1.98 ng m^{-3}, Fu et al., 2012a) and Mt. Changbai (1.60 ± 0.51 ng m^{-3}, Fu et al., 2012b) and regional background levels (2.94 ± 2.02 ng m^{-3}, Li et al., 2011; 2.50 ± 1.50 ng m^{-3}, Dou et al., 2013), were slightly lower than those of urban areas in China, such as Beijing (2.1–45.2 ng m^{-3}, Wang et al., 2007), Nanjing (7.9 ± 7.0 ng m^{-3}, Zhu et al., 2012), Shanghai (7.79 ± 3.29 ng m^{-3}, Zhang et al., 2011a), Changchun (18.4 ng m^{-3}, Fang et al., 2004) and Guiyang (8.40 ± 4.87 ng m^{-3}, Feng et al., 2004). Overall, higher TGM concentrations have been observed at urban sites located in southwestern China, followed by the northern and southeastern regions. In a study by Zhu et al. (2012), a comprehensive overview of TGM concentrations in other countries and regions is available. Compared with the TGM in other countries, the level in the PRD is similar to other developing (such as Mexico) and East Asian countries (such as Korea); however, the levels in urban China are significantly elevated compared to values observed at global sites in Europe and North America.

A recent study conducted for only one month (2008.11.23–2008.12.22) in a rural area of the Guangzhou reported a TGM

concentration of 2.94 ng m^{-3} (Fig. 1, Li et al., 2011), which is obviously lower compared to the same month in our study (6.08 ± 1.82 ng m^{-3}). However, the TGM levels in our study were significantly lower compared to those of a study performed in 2005 in the Guangzhou urban region (13.5 ± 7.1 ng m^{-3}) (Wang et al., 2007). These results may indicate that mercury levels in the atmosphere of Guangzhou city have been declining after several decades of pollution control and prevention. The Chinese government has taken a series of vigorous measures to control atmospheric pollution since 2007, including shutting down small power plants with unit capacities less than 50,000 kW and small cement plants. In addition, the 16th Asian Games was held in Guangzhou in 2010, and a number of manufacturing plants with high energy consumption and emission rates were closed. An obvious trend for decreasing SO_2 and NO_2 concentrations was observed from 2005 to 2012 (HKEPD, 2012). The measures of desulfurisation and denitrification resulted in a synergistic effect that decreased atmospheric mercury emissions. Simultaneously, the utilisation of clean energy also reduced anthropogenic mercury emissions (Zheng et al., 2011; Cheng and Hu, 2012).

Although the DH site is located within a nature reserve, most of the regional large point sources (e.g., coal-fired power, cement, iron and steel plants) are situated upstream of the annual predominant wind directions (northeasterly and southeasterly, accounting for 47.2% and 20.9%, respectively) (Figs. 1 and 4). Most pollutants from numerous anthropogenic emission sources in the PRD, especially mercury, are easily transferred to the DH site by wind (Fig. 1), which account for the high TGM levels at this site. The difference between the two sites for the same months was investigated using the TGM-level *t* test. The results indicated no significant difference ($p = 0.421$), which suggests that TGM pollution in the PRD area may be regional and even. In fact, regional atmospheric pollution in the PRD has been previously described and reported (Zhang et al., 2008b, 2011b). Simultaneously, a wide variation range of TGM at the two monitoring sites indicates that they were influenced by the surrounding anthropogenic emission sources, except for mercury released from the ground (Lee et al., 1998).

We observed an interesting phenomenon at the DH site. The TGM levels obviously declined during the traditional Chinese Spring Festival (2010.2.10–2010.3.9) (3.33 ± 1.04 ng m^{-3}); however, the values were 6.32 ± 1.67 ng m^{-3} and 5.07 ± 0.33 ng m^{-3} before and after the Spring Festival, respectively. Similarly, at the GZ site, the TGM concentrations observed before and after the Spring Festival were 4.66 ± 1.92 ng m^{-3} and 4.79 ± 1.35 ng m^{-3}, respectively, with a value of 4.26 ± 0.89 ng m^{-3} observed during this period (2011.1.17–2011.2.16) (Fig. 2). Due to the factory shut down or reduced production during the Spring Festival, power demand for Guangdong province displays an obvious trough during this period each year (Luo et al., 2007). The trend in the TGM variation was consistent with the power demand, suggesting that atmospheric mercury emissions in the PRD are associated with power generation.

3.2. Seasonal distribution and fluctuation pattern of TGM

At the DH site, the seasonal variation of the TGM concentrations in descending order was spring (5.50 ng m^{-3}), winter (5.48 ng m^{-3}), and autumn (3.95 ng m^{-3}). The results of the TGM level *T* test indicated that there were significant differences between autumn and the other two seasons ($p < 0.001$) and no significant differences between spring and winter ($p = 0.323$). Similar to the DH site, the TGM levels at the GZ site were higher in spring (5.21 ng m^{-3}), followed by winter (4.4 ng m^{-3}), autumn (4.3 ng m^{-3}) and summer (4.16 ng m^{-3}) (Fig. 3). There were significant differences between spring and the other three seasons ($p < 0.001$), but no significant differences between summer, autumn and winter ($p > 0.1$). Overall, higher TGM levels were observed in spring at both sites, which indicates the mercury pollution is more serious during the spring in the PRD. A high daily mean TGM concentration was also found in the spring, including the highest value of 29.94 ng m^{-3} on April 9 at the DH site.

At the DH site, the seasonal fluctuation of TGM was smallest in autumn (SD = 1.21 ng m^{-3}) and significantly larger in the spring and winter (SD = 4.11, 2.41 ng m^{-3}). At the GZ site, the seasonal fluctuation of TGM was relatively small during all four seasons (SD = 1.25, 1.21, 0.97, 1.61 ng m^{-3} in spring, summer, autumn and winter, respectively). It was noted that similar seasonal fluctuation trends were found at the two monitoring sites. In the PRD, the fluctuation in the TGM level in autumn was relatively stable, whereas it was relatively greater in spring and winter.

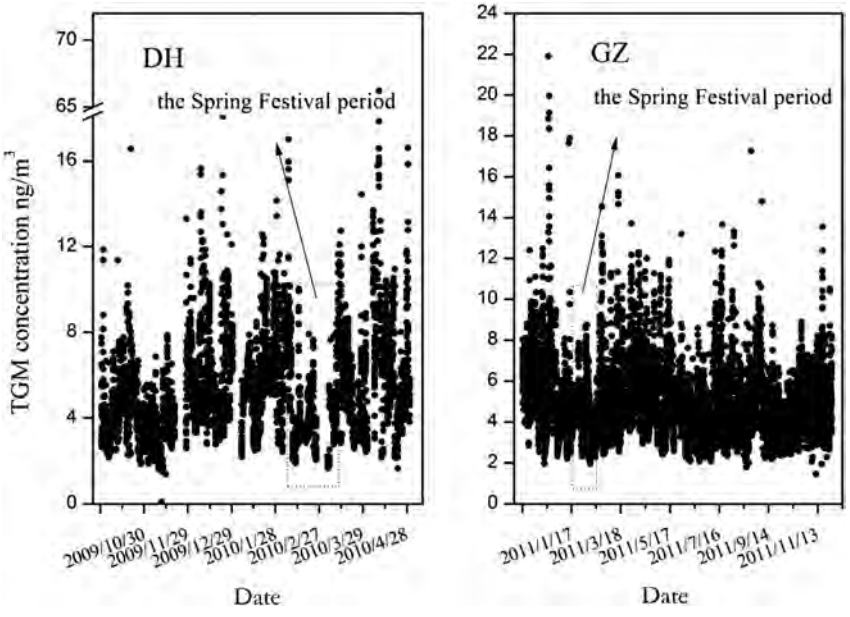

Fig. 2. Time series of TGM using 1 h averages in the Dinghu Mountain area and in Guangzhou.

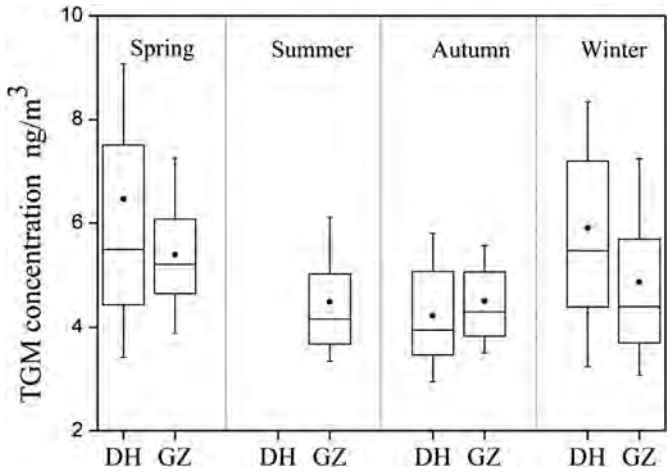

Fig. 3. Seasonal variation of total gaseous mercury in the Dinghu Mountain area and in Guangzhou. Boxed horizontal solid lines show the 25th, 50th, and 75th percentiles, the black dots within each box indicate the mean TGM concentration, and the whiskers represent the 10th and 90th percentiles of the TGM concentration.

Because of the lack of a heating period in the PRD, the amounts of energy consumed during different seasons remain basically invariable. This same seasonal distribution and fluctuation pattern in the PRD should be primarily related to meteorological factors (Huang et al., 2009). In the PRD, the prevailing strong wind directions during the summer and winter are clean air mass by the southeasterly monsoon wind from the South Sea and air mass by the northeasterly monsoon wind from the Siberian High, respectively (Wang et al., 2003). Fu et al. (2010) indicated that the summer monsoon may affect the seasonal distribution of TGM in South China. Spring is the transitional period between the winter and summer monsoons, with the prevailing wind changing from north to southeast monsoon winds (Wang et al., 2003). When the intensities between the warm air from the South China Sea and the cold and dry air flow from the north are equivalent, temperature inversion (frontal inversion) and hazy weather appear during the spring in the PRD (Fan et al., 2006). The average visibility and relative humidity were 7040 m and 72%, respectively, in the spring, suggesting the appearance of hazy weather. Under these meteorological conditions, poor air dispersion can lead to high TGM levels in the spring. In addition, some study results have indicated that the relationship between the TGM level and wind speed is significant and that atmospheric mercury from local emission sources could accelerate diffusion with increasing wind speeds (Wan et al., 2009). The seasonal average wind speeds at GZ were 1.63, 1.85, 1.25 and 1.26 m s^{-1}, respectively, during spring, summer, autumn and winter, and at DH were 1.21, 1.80, 1.40, 1.20 m s^{-1}, respectively. In this study, the TGM levels and wind speeds at the DH and GZ sites displayed a significant negative correlation ($r = -0.29$, $p < 0.001$; $r = -0.459$, $p < 0.001$). Generally, different seasonal monsoon wind directions (different mercury levels carried by different air masses) and wind speeds primarily lead to a seasonal distribution pattern of TGM. Of course, the low mercury concentration may be partially attributable to the increased height of the atmospheric boundary layer or be oxidised by high O_3 and OH· levels during periods of high temperatures during the summer and autumn. However, the change in the wind direction during the spring leads to a large fluctuation of the TGM. Moreover, the Chinese traditional Spring Festival occurs in the winter, and it is reasonable to assume that the wide TGM fluctuation in winter was related to the low power demand (see Section 3.1).

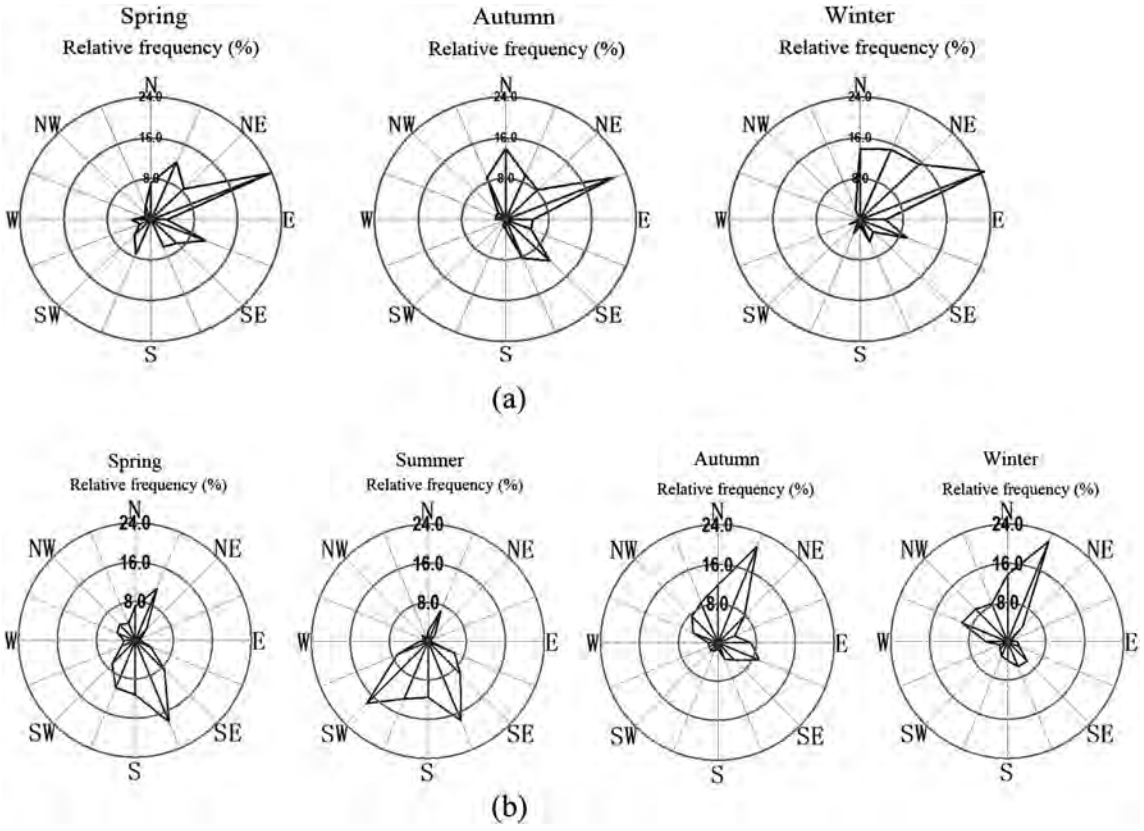

Fig. 4. Seasonal frequency distribution of the wind directions for: (a) Dinghu Mountain area; (b) Guangzhou.

3.3. Diurnal pattern of TGM in the PRD

The TGM concentrations at the two sites exhibited a pronounced diurnal pattern (Fig. 5), which were averaged over each hour of the entire study period. At the DH site, the TGM levels during the daytime (06:00–18:00) and nighttime (18:00–06:00) periods were 5.84 and 5.34 ng m^{-3}, respectively. The TGM concentrations reached a maximum at 10:00 in the morning and a minimum at 00:00 at night (Fig. 5). This diurnal pattern was of the daytime-dominant type, in agreement with some other studies, such as those conducted at Mt. Gongga, Mt. Changbai and Mt. Lulin (Fu et al., 2008; Wan et al., 2009; Sheu et al., 2010). However, this pattern is significantly different from that at Mt. Waliguan, a Global Atmospheric Watch Baseline Station in China (Fu et al., 2012a). A high level of mercury from anthropogenic sources was transported upslope from the foot of a mountain by valley wind in the daytime. In the nighttime, the TGM level decreased due to mountain wind carrying clear air (Fu et al., 2008; Wan et al., 2009; Sheu et al., 2010). The daily TGM pattern at the DH site may be related to variations between daytime and nighttime winds. Theoretically, another possible explanation is that the temperature and solar radiation were dominant factors in the morning (before 10:00) and enhanced the mercury release from the ground surface. However, as the temperature increased further, the boundary layer height increase resulted in the mercury decrease. In contrast to the TGM levels during the daytime and nighttime at the DH site, those at the GZ site were 4.72 and 5.16 ng m^{-3}, respectively. This pattern was nighttime-dominant, with two peak values in TGM observed at 7:00 and 22:00 and a minimum value at 14:00 in the afternoon. In previous studies, high mercury concentrations in the morning and their depletion in the mid-afternoon have been observed in Chinese cities, such as Guiyang (Feng et al., 2004), Changchun (Fang et al., 2004) and Guangzhou (Wang et al., 2007), and in other overseas cities, e.g., Seoul, South Korea (Kim et al., 2005; Choi et al., 2009), a suburban area of France (Dommergue et al., 2002), Reno, USA (Stamenkovic et al., 2007) and Harwell, England (Lee et al., 1998). During the night, the TGM concentrations in the ambient air of the industrial and urban areas likely increased due to the significant mercury emissions under shallow nocturnal boundary layer conditions (Lee et al., 1998; Feng et al., 2004). The diurnal-varied pattern of TGM in Guangzhou is in agreement with the daily variation of the boundary-layer height (Zhang et al., 2008a). As evident in Fig. 6, the daily TGM levels and O_3 concentrations

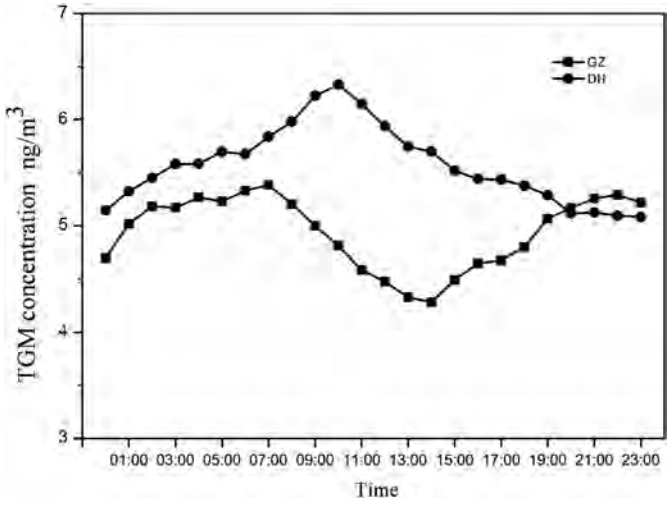

Fig. 5. Average diel variation of total gaseous mercury in the Dinghu Mountain area and in Guangzhou.

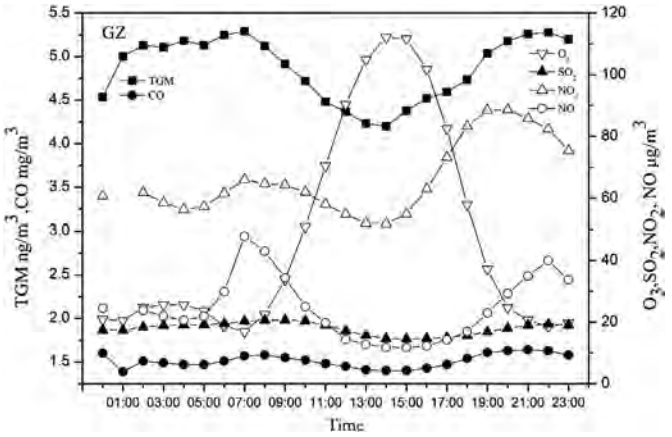

Fig. 6. Average diel variation of TGM, SO_2, NO_2, NO, CO and O_3 levels in Guangzhou.

were significantly negatively correlated in Guangzhou ($r = -0.903$, $p < 0.001$). These results suggest that the diurnal distribution pattern of TGM in Guangzhou was controlled by variations in the boundary layer and O_3 concentrations. The varied trends of TGM at the DH and GZ sites were the same and tended to increase between 00:00 and 07:00. A sudden increase in TGM between 6:00 and 7:00 could be due to the activation of local surface emission sources in the morning with the sunrise and increased temperatures (Stamenkovic et al., 2007; Li et al., 2011).

3.4. Relationship between TGM and criteria pollutants

Coal combustion is an important emission source of atmospheric SO_2, NO_2 and mercury. The combustion of fossil fuels (primarily coal) in stationary combustion facilities represents 35% of the total amount of anthropogenic sources (Pirrone et al., 2010). The relationships between the SO_2, NO_2 and TGM data have been commonly used to identify mercury emission sources (Lee et al., 1998). As shown in Fig. 7, during the monitoring period, similar varied trends and significant correlations were found between the daily TGM level and the SO_2 and NO_2 ($r = 0.36$, $p < 0.001$; $r = 0.29$, $p < 0.001$) at the DH site. In the PRD, the largest emission sources for SO_2 and NO_2 are fossil fuel combustion (particularly coal combustion). This result may account for the relationship between TGM and SO_2 and NO_2 levels at the DH site. According to our previous discussion (section 3.2), energy supply in the PRD is primarily dependent on coal, and trends in energy demand are similar to the variations in the TGM level, which further confirms the significant relationship between TGM levels and mercury emissions from coal combustion.

The daily TGM level and NO, NO_2 and CO levels at the GZ site were significantly positively related ($r = 0.501$, $p < 0.001$; $r = 0.579$, $p < 0.001$; $r = 0.358$, $p < 0.001$). The TGM, NOx and CO had two major peaks at rush hour (7:00–9:00, AM; 19:00–21:00, PM) (Fig. 6). The correlations with NOx and CO, but not SO_2, may suggest that vehicle exhaust emission is an important source of mercury, which agrees with results found at Nanjing and Shanghai in China (Friedli et al., 2011; Zhu et al., 2012). Vehicle exhaust emission has been considered an important emission source for mercury (Conaway et al., 2005; Landis et al., 2007; Won et al., 2007). In 2011, the motor vehicle population was over 2.3 million in Guangzhou (GTRI, 2012). No correlation was observed between the daily TGM level and the SO_2 level from the annual data at the GZ site ($r = 0.096$, $p = 0.8$); however, inverse results were observed in June and August, with significant positive correlations ($r = 0.469$, $p = 0.009$; $r = 0.564$, $p = 0.003$) (Fig. 7). The prevailing winds in

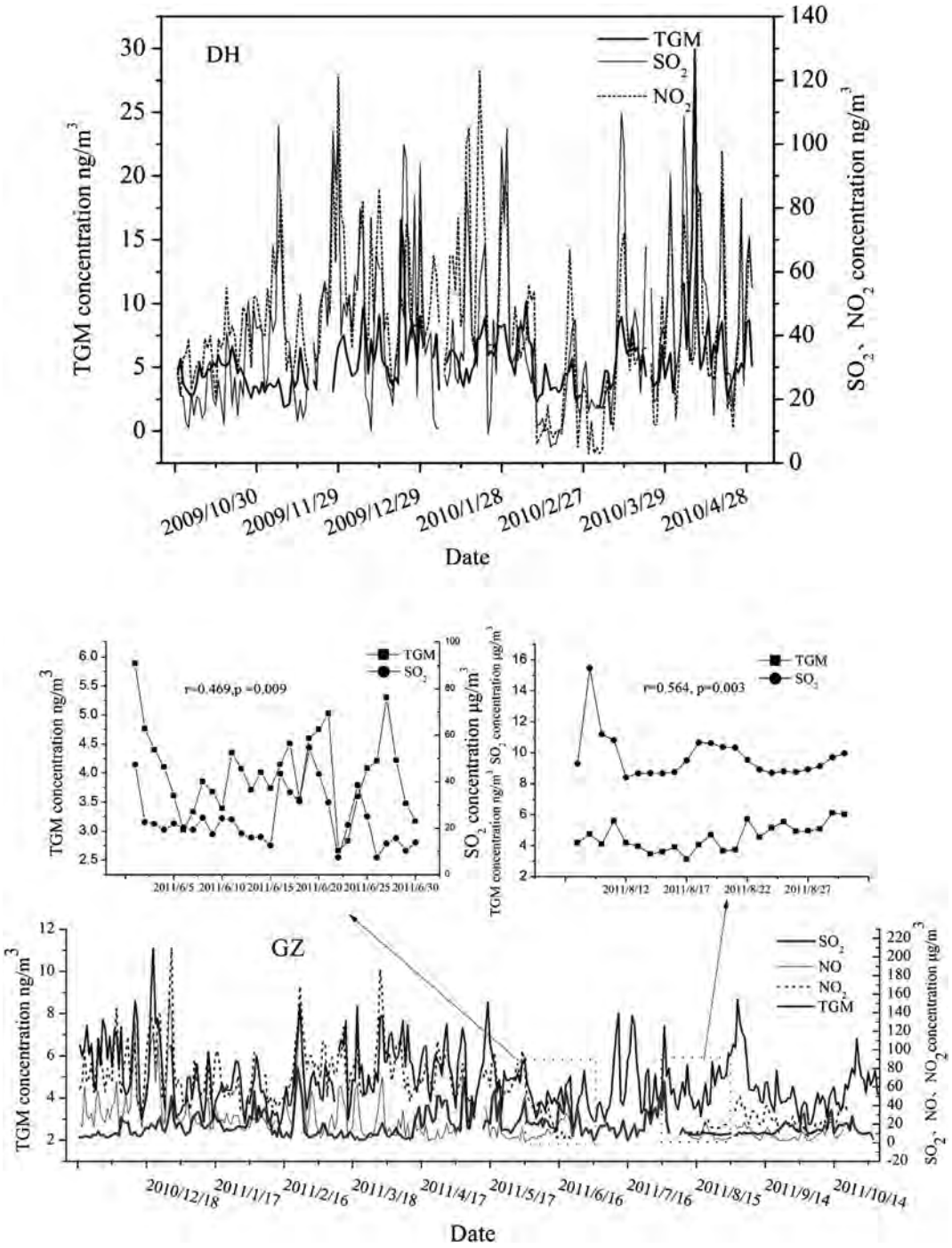

Fig. 7. Time series of TGM, SO_2, NO and NO_2 levels in the Dinghu Mountain area and in Guangzhou.

June and August were southeasterly (56.6%) and southwesterly (58.9%), respectively, and could well explain the above exceptions, i.e., there are many coal-fired power plants in the two directions (Fig. 1). As a whole, TGM in Guangzhou city may be influenced by both vehicle exhaust emission and coal-fired power plants.

3.5. Potential sources of TGM in the PRD

As previously discussed, the PRD region is polluted by mercury. To further identify potential sources of TGM, potential industrial emission sources (e.g., coal-fired power, cement, ceramic and iron and steel plants) are presented in Fig. 1. Numerous anthropogenic mercury emission sources surround the DH site. A northeasterly wind is the prevailing wind direction, followed by southeasterly winds (Fig. 8a). Thus, the observed elevated TGM levels indicate the potential influence of high mercury emissions from southeastern and northeastern areas (Fig. 8b). According to the location of the sampling site and the wind direction, the DH site is primarily affected by anthropogenic emission sources from the entire PRD region.

For the GZ site, the figures for the TGM concentrations indicate that high TGM levels were carried by the wind from all directions

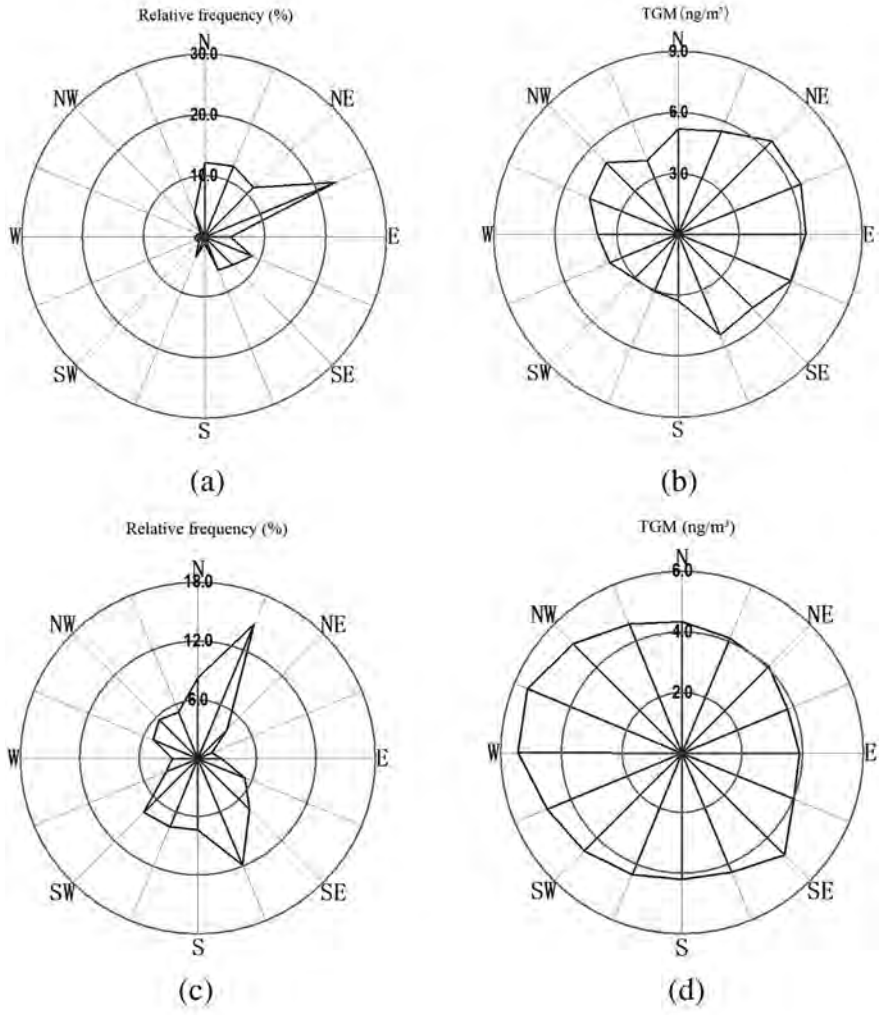

Fig. 8. Frequency distribution of the wind directions and the mean distribution of TGM during the measurement campaigns for: (a), (b) Dinghu Mountain area; (c), (d) Guangzhou.

(Fig. 8d), in agreement with the distribution of the surrounding emission sources (Fig. 1). Although northeasterly wind was dominant at the GZ monitoring site (Fig. 8c), it carried a relatively low concentration of TGM. However, the non-dominant northwesterly and secondary prevailing southeasterly winds carried high TGM levels. These results suggest that stronger anthropogenic emission sources are obviously located in southeastern and northwestern directions from the GZ monitoring site. The enhanced TGM levels may be due to local anthropogenic emission sources (see Section 3.4). A large coal-fired power plant is located southeast of the GZ site. In addition, a coal-fired power plant, numerous cement plants and city centre (containing a large number of motor vehicles) are located northwest of the GZ site (Fig. 1), which are major anthropogenic mercury emission sources (Pirrone et al., 2010), and these point source and mobile source emissions result in higher mercury concentrations. Moreover, our study on the mercury in the PRD soil also indicates that an area highly polluted with mercury is situated close to the GZ monitoring site (Chen et al., 2012).

4. Conclusions

The annual average TGM value in the PRD is significantly greater than the background values in the Northern Hemisphere. These results indicate that the atmosphere in this region has suffered from mercury pollution, indicating a regionalisation effect. Compared with several years ago, some pollutant control measures applied by local governments have led to obvious decreases in atmospheric mercury levels. Seasonal variations in the TGM at the two sites were similar, with a descending order of spring, winter, autumn and summer. Monsoons were the dominant factor controlling the seasonal variation of TGM at the DH and GZ, with variations in the boundary layer and oxidation possibly partially contributing. The daily TGM distribution patterns at the two sites were obviously different. At the DH site, a regional monitoring site, the TGM during the daytime was higher than at nighttime and was primarily influenced by mountain and valley winds. At the GZ site, an urban monitoring site, the TGM distribution pattern was the opposite and was primarily influenced by the boundary-layer height and O_3 concentration. The relationships between TGM and criteria pollutants (SO_2, CO, NO_x) at the two monitoring sites were different. At the DH site, a significant correlation between TGM, SO_2 and the energy demand was found, suggesting coal-fired emission as an important source of mercury for this regional monitoring site. However, at the GZ site, significant correlations between TGM and CO and partially TGM and SO_2 may suggest that combined vehicle exhaust emissions and coal combustion are the dominant mercury

sources for this urban monitoring site. The TGM distribution figure, which is related to the wind-rose pattern and the distribution figure of emission sources, indicate significant contributions from anthropogenic emission sources.

The subtropical monsoon climate in the PRD can accelerate the material cycle among different environmental media. Mercury entering the environment can be converted to a methylated mercury species through a variety of abiotic and biotic processes. Subtle health effects may be observed because of the possible high dietary intake of methylated mercury due to dietary habits that include excessive fish consumption. National and local governments should take significant efforts to control mercury pollution in this region.

Acknowledgements

This study was funded by the Commonwealth and Environmental Protection Project of the Ministry of Environmental Protection of the People's Republic of China (MEP) (No. 200809011), Special Scientific Research Funds for Environmental Protection Commonweal Section (zx_200910_25) and the National Science Foundation of China (No. 41105082). Dr Xuewu Fu from the Institute of Geochemistry of Chinese Academy of Sciences reviewed and revised the manuscript.

References

Chen, L., Xu, Z., Ding, X., Zhang, W., Huang, Y., Fan, R., Sun, J., Liu, M., Qian, D., Feng, Y., 2012. Spatial trend and pollution assessment of total mercury and methylmercury pollution in the Pearl River Delta soil, South China. Chemosphere 88, 612–619.

Chen, L., Liu, M., Fan, R., Ma, S., Xu, Z., Ren, M., He, Q., 2013. Mercury speciation and emission from municipal solid waste incinerators in the Pearl River Delta, South China. Science of the Total Environment 447, 396–402.

Cheng, H.F., Hu, Y.N., 2012. Mercury in municipal solid waste in China and Its Control: a Review. Environmental Science and Technology 46, 593–605.

Choi, E.M., Kim, S.H., Holsen, T.M., Yi, S.M., 2009. Total gaseous concentrations in mercury in Seoul, Korea: local sources compared to long-range transport from China and Japan. Environmental Pollution 157, 816–822.

Ci, Z.J., Zhang, X.S., Wang, Z.W., Niu, Z.C., 2011. Atmospheric gaseous elemental mercury (GEM) over a coastal/rural site downwind of East China: temporal variation and long-range transport. Atmospheric Environment 45, 2480–2487.

Conaway, C.H., Mason, R.P., Steding, D.J., Flegal, A.R., 2005. Estimate of mercury emission from gasoline and diesel fuel consumption, San Francisco Bay area, California. Atmospheric Environment 39, 101–105.

Dastoor, A.P., Larocque, Y., 2004. Global circulation of atmospheric mercury: a modeling study. Atmospheric Environment 38, 147–161.

Dommergue, A., Ferrari, C.P., Planchon, F.A.M., Boutron, C.F., 2002. Influence of anthropogenic sources on total gaseous mercury variability in grenoble suburban air (France). Science of Total Environment 297, 203–213.

Dou, H.Y., Wang, S.X., Wang, L., Zhang, L., Hao, J.M., 2013. Characteristics of total gaseous mercury concentrations at a rural site of Yangtze Delta, China. Environmental Science 34, 1–7 (in Chinese).

Fan, S.J., Wang, A.Y., Fan, Q., Liu, J., Wang, B.M., 2006. Atmospheric boundary layer features of Pearl River Delta and its conception model. China Environmental Science 26, 4–6 (in Chinese).

Fang, F., Wang, Q., Li, J., 2004. Urban environmental mercury in Changchun, a metropolitan city in Northeastern China: source, cycle, and fate. Science of the Total Environment 330, 159–170.

Feng, X.B., Shang, L.H., Wang, S.F., Tang, S.L., Zheng, W., 2004. Temporal variation of total gaseous mercury in the air of Guiyang, China. Journal of Geophysical Research 109, D03303. http://dx.doi.org/10.1029/2003JD004159.

Friedli, H.R., Arellano, A.F., Geng, F., Cai, C., Pan, L., 2011. Measurements of atmospheric mercury in Shanghai during September 2009. Atmospheric Chemistry and Physics 11, 3781–3788.

Fu, X.W., Feng, X.B., Zhu, W.Z., Wang, S.F., Lu, J.L., 2008. Total gaseous mercury concentrations in ambient air in the eastern slope of Mt. Gongga, South-Eastern fringe of the Tibetan plateau, China. Atmospheric Environment 42, 970–979.

Fu, X.W., Feng, X.B., Wang, S.F., Rothenberg, S., Shang, L.H., Li, Z.G., Qiu, G.L., 2009. Temporal and spatial distributions of total gaseous mercury concentrations in ambient air in a mountainous area in southwestern China: implications for industrial and domestic mercury emissions in remote areas in China. Science of the Total Environment 407, 2306–2314.

Fu, X.W., Feng, X.B., Zhang, G., Xu, W.H., Li, X.D., Yao, H., Liang, P., Li, J., Sommar, J., Yin, R.S., Liu, N., 2010. Mercury in the marine boundary layer and seawater of the South China Sea: concentrations, sea/air flux, and implication for land outflow. Journal of Geophysical Research 115, D06303. http://dx.doi.org/10.1029/2009JD012958.

Fu, X.W., Feng, X.B., Liang, P., Deli-Geer, Zhang, H., Ji, J., Liu, P., 2012a. Temporal trend and sources of speciated atmospheric mercury at Waliguan GAW station, Northwestern China. Atmospheric Chemistry and Physics 12, 1951–1964.

Fu, X.W., Feng, X., Shang, L.H., Wang, S.F., Zhang, H., 2012b. Two years of measurements of atmospheric total gaseous mercury (TGM) at a remote site in Mt. Changbai area, Northeastern China. Atmospheric Chemistry and Physics 12, 4215–4226.

Guangzhou Transports Research Institute (GTRI), September, 4 2012. White Paper of Guangzhou Transport Development.

Guangdong Statistical Yearbook, 2009 (accessed August 2009). http://www.gdstats.gov.cn/tjnj/2009/mlc.htm.

Hong Kong Environmental Protection Department (HKEPD), 2012. Pearl River Delta Regional Air Quality Monitoring Report (accessed October 2012). <http://www.epd.gov.hk/epd/english/resources_pub/publications/m_report. html>.

Huang, D.Y., Xu, Y.G., Peng, P.A., Zhang, H.H., Lan, J.B., 2009. Chemical composition and seasonal variation of acid deposition in Guangzhou, South China: comparison with precipitation in other major Chinese cities. Environmental Pollution 157, 35–41.

Kim, K.H., Ebinghaus, R., Schroeder, W.H., Blanchard, P., Kock, H.H., Steffen, A., Froude, F.A., Kim, M.Y., Hong, S.M., Kim, J.H., 2005. Atmospheric mercury concentrations from several observatory sites in the northern hemisphere. Journal of Atmospheric Chemistry 50, 1–24.

Landis, M.S., Lewisa, C.W., Stevens, R.K., Keeler, G.J., Dvonch, J.T., Tremblay, R.T., 2007. Ft. McHenry tunnel study: source profiles and mercury emissions from diesel and gasoline powered vehicles. Atmospheric Environment 41, 8711–8724.

Lee, D.S., Dollard, G.J., Pepler, S., 1998. Gas-phase mercury in the atmosphere of the United Kingdom. Atmospheric Environment 32, 855–864.

Li, Z., Xia, C.H., Wang, X.M., Xiang, Y.R., Xie, Z.Q., 2011. Total gaseous mercury in Pearl River Delta region, China during 2008 winter period. Atmospheric Environment 45, 834–838.

Lindberg, S., Bullock, R., Ebinghaus, R., Engstrom, D., Feng, X., Fitzgerald, W., Pirrone, N., Prestbo, E., Seigneur, C., 2007. A synthesis of progress and uncertainties in attributing the sources of mercury in deposition. Ambio 36, 19–32.

Luo, S.B., Ji, Z.P., Ma, Y.H., Luo, X.M., Zeng, Q., Lin, S.B., 2007. The variability characteristics and prediction of Guangdong electrical load during 2002-2004. Journal of Tropical Meteorology 23, 153–161 (in Chinese).

Pacyna, E.G., Pacyna, J.M., Sundseth, K., Munthe, J., Kindbom, K., Wilson, S., Steenhuisen, F., Maxson, P., 2010. Global emission of mercury to the atmosphere from anthropogenic sources in 2005 and projections to 2020. Atmospheric Environment 44, 2487–2499.

Pirrone, N., Cinnirella, S., Feng, X., Finkelman, R.B., Friedli, H.R., Leaner, J., Mason, R., Mukherjee, A.B., Stracher, G., Streets, D.G., Telmer, K., 2009. Global Mercury Emissions to the Atmosphere from Natural and Anthropogenic Sources. Springer, New York, USA, pp. 3–49.

Pirrone, N., Cinnirella, S., Feng, X., Finkelman, R.B., Friedli, H.R., Leaner, J., Mason, R., Mukherjee, A.B., Stracher, G.B., Streets, D.G., Telmer, K., 2010. Global mercury emissions to the atmosphere from anthropogenic and natural sources. Atmospheric Chemistry and Physics 10, 5951–5964.

Seigneur, C., Vijayaraghavan, K., Lohman, K., Karamchandani, P., Scott, C., 2004. Global source attribution for mercury deposition in the United States. Environmental Science and Technology 38, 555–569.

Sheu, G.R., Lin, N.H., Wang, J.L., Lee, C.T., Ou, C.F., Wang, S.H., 2010. Temporal distribution and potential sources of atmospheric mercury measured at a high-elevation background station in Taiwan. Atmospheric Environment 44, 2393–2400.

Shi, J.B., Carman, C.M., Zhang, G., Jiang, G.B., Li, X.D., 2010. Mercury profiles in sediments of the Pearl River Estuary and the surrounding coastal area of South China. Environmental Pollution 158, 1974–1979.

Stamenkovic, J., Lyman, S., Gustin, M.S., 2007. Seasonal and diel variation of atmospheric mercury concentrations in the Reno (Nevada, USA) airshed. Atmospheric Environment 41, 6662–6672.

Streets, D.G., Hao, J.M., Wu, Y., Jiang, J.K., Chan, M., Tian, H.Z., Feng, X.B., 2005. Anthropogenic mercury emissions in China. Atmospheric Environment 39, 7789–7806.

United Nations Environment Programme (UNEP), 2002. Global Mercury Assessment. UNEP-Chemicals, Gevena, Switzerland.

Valente, R.J., Shea, C., Humes, K., Tanner, R.L., 2007. Atmospheric mercury in the Great Smoky Mountains compared to regional and global levels. Atmospheric Environment 41, 1861–1873.

Wan, Q., Feng, X.B., Lu, J.L., Zheng, W., Song, X.J., Han, S.J., Xu, H., 2009. Atmospheric mercury in Changbai Mountain area, northeastern China I: the seasonal distribution pattern of total gaseous mercury and its potential sources. Environmental Research 109, 201–206.

Wang, T., Ding, A.J., Blake, D.R., Zahorowski, W., Poon, C.N., Li, Y.S., 2003. Chemical characterization of the boundary layer outflow of air pollution to Hong Kong during February–April 2001. Journal of Geophysical Research 108 (D20), 8787.

Wang, Z.W., Chen, Z.S., Duan, N., Zhang, X.S., 2007. Gaseous elemental mercury concentration in atmosphere at urban and remote sites in China. Journal of Environmental Sciences 19, 176–180.

Won, J.H., Park, J.Y., Lee, T.G., 2007. Mercury emissions from automobiles using gasoline, diesel and LPG. Atmospheric Environment 41, 7547–7552.

Wong, C.S.C., Duzgoren-Aydin, N.S., Aydin, A., Wong, M.H., 2006. Sources and trends of environmental mercury emissions in Asia. Science of the Total Environment 368, 649–662.

Yang, Y.J., Wang, Y.S., Wen, T.X., Zhao, Y.N., Li, J., 2009. Element characteristics and sources of PM2.5 at Mount Dinghu in 2006. Environmental Science 30, 988–992 (in Chinese).

Yu, W., Luo, X.Y., Fan, S.J., Liu, J., Feng, Y.R., Fan, Q., 2011. Characteristics analysis and numerical simulation study of a severe air pollution episode over the Pearl River Delta. Research of Environmental Sciences 24, 645–653 (in Chinese).

Zhang, Y.H., Su, H., Zhong, L.J., Cheng, Y.F., Zeng, L.M., Wang, X.S., Xiang, Y.R., Wang, J.L., Gao, D.F., Shao, M., Fan, S.J., Liu, S.C., 2008a. Regional ozone pollution and observation based approach for analyzing ozone-precursor relationship during the PRIDE-PRD 2004 campaign. Atmospheric Environment 42, 6203–6218.

Zhang, Y.H., Hua, M., Zhong, L.J., Wiedensohler, A., Liu, S.C., Andreae, M.O., Wang, W., Fang, S.J., 2008b. Regional integrated experiments on air quality over Pearl River Delta 2004 (PRIDE-PRD2004): overview. Atmospheric Environment 42, 6157–6173.

Zhang, Y.Y., Xiu, G.L., Zhang, D.N., Zhang, M.G., Zhang, R.J., 2011a. Total gaseous mercury in ambient air of shanghai: its seasonal variation in relation to meteorological condition. Environmental Science &Technology 34, 155–158 (in Chinese).

Zhang, Y.N., Xiang, Y.R., Chan, L.Y., Chan, C.Y., Sang, X.F., Wang, R., Fu, H.X., 2011b. Procuring the regional urbanization and industrialization effect on ozone pollution in Pearl River Delta of Guangdong, China. Atmospheric Environment 45, 4898–4906.

Zheng, J.Y., Ou, J.M., Mo, Z.W., Yin, S.S., 2011. Mercury emission inventory and its spatial characteristics in the Pearl River Delta region, China. Science of the Total Environment 412–413, 214–222.

Zhu, J., Wang, T., Talbot, R., Mao, H., Hall, C.B., Yang, X., Fu, C., Zhuang, B., Li, S., Han, Y., Huang, X., 2012. Characteristics of atmospheric total gaseous mercury (TGM) observed in urban Nanjing, China. Atmospheric Chemistry and Physics 12, 12103–12118.